

# Modified Opposite-Spin-Scaled Double-Hybrid Functionals

Golokesh Santra<sup>\*, 1, a)</sup>, Markus Bursch<sup>\*, 2, 3, a)</sup> and Lukas Wittmann<sup>\*3, a)</sup>

<sup>1)</sup>Max-Planck-Institut für Kohlenforschung, Kaiser-Wilhelm-Platz 1, 45470 Mülheim an der Ruhr, Germany

<sup>2)</sup>FACCT's GmbH, 50677, Köln, Germany

<sup>3)</sup>Mulliken Center for Theoretical Chemistry, Universität Bonn, Beringstr. 4, 53115 Bonn, Germany

(\*Electronic mail: wittmann@thch.uni-bonn.de)

(\*Electronic mail: bursch@thch.uni-bonn.de)

(\*Electronic mail: santra@kofo.mpg.de)

(Dated: 27 August 2024)

We investigate the potential performance improvements of double-hybrid density functionals by replacing the standard opposite-spin-scaled MP2 (SOS-MP2) with the modified opposite-spin-scaled MP2 (MOS-MP2) in the nonlocal correlation component. Using the large and diverse GMTKN55 dataset, we find that MOS-double hybrids provide significantly better accuracy compared to SOS-MP2-based double hybrids when empirical dispersion correction is not employed. The non-covalent interaction subsets account for the majority of this improvement. Adding the DFT-D4 dispersion correction to MOS-type double hybrids does not provide any superior performance over conventional dispersion-corrected SOS-MP2-based double hybrids. Nevertheless, for nine tested transition metal sets, dispersion-corrected spin-component-scaled (SCS) double hybrids are still significantly better than any MOS-double hybrid functional.

## I. INTRODUCTION

Kohn–Sham density functional theory (DFT) is one of the main cornerstones of modern computational chemistry, valued for its ability to achieve a good balance between accuracy and computational efficiency, especially with increasing system size.<sup>1,2</sup> Perdew’s *Jacob’s Ladder*<sup>3</sup> categorizes density functionals based on the type of density or orbital information they utilize within the approximation. Each ascending rung on the ladder is believed to offer greater accuracy than the one before it, though this improvement typically comes with increased computational cost. The highest, fifth rung, is represented by the so-called double-hybrid (DH) functionals that include both, an admixture of Hartree–Fock exchange (HFX) and a wavefunction theory-based correlation contribution into the density functional formulation. The latter is usually computed by second-order perturbation theory (PT2), with second-order Møller–Plesset theory (MP2) being the most prominent method of choice.<sup>4–9</sup>

Despite the popularity of MP2 as a component of DHs, it suffers from systematic problems, such as its divergent behavior for small orbital energy gaps and the systematic underestimation of long-range dispersion interactions.

The first problem can be addressed by replacing simple MP2 with the direct random phase approximation<sup>10</sup> (dRPA) correlation or by regularizing the MP2 energy expression, e.g., using the  $\kappa$ -regularization scheme proposed by Shee *et al.*<sup>11</sup> In a recent study, we showed that dispersion-corrected dRPA-based double hybrids are only as good as MP2-based double hybrids for main group chemistry problems, while dRPA-based double hybrids perform significantly better for

metal-organic barrier heights.<sup>12</sup> The second possibility has also been investigated for the double-hybrid functionals.<sup>13,14</sup> Martin and coworkers have shown that for typical double hybrids, which usually employ a large percentage ( $\sim 70\%$  or higher) of HF-exchange, using  $\kappa$ -MP2 correlation instead of canonical MP2 has no extra benefit.<sup>13</sup> The regularized DHs are better than their standard counterparts, only if a smaller percentage of HF-exchange ( $\sim 50\%$ ) is used without the spin-component scaling of the MP2 energy. In a more recent study, Wittmann *et al.* have found that  $\kappa$ Pr<sup>2</sup>SCAN50, employing only 50% HFX, performs marginally better overall than the regular Pr<sup>2</sup>SCAN50, while improving performance for small orbital-energy gap systems and thus adding a layer of robustness for such systems.<sup>14</sup>

The second problem is often addressed by adding a dispersion correction to the total electronic energy. This is a common issue with many density functional approximations (DFAs), as they often fail to accurately describe long-range correlation effects, leading to a systematic underestimation of London dispersion interactions. As double hybrids usually contain a scaled-down portion of MP2 correlation, they also suffer from a similar issue; therefore, additional London dispersion corrections are required. Some popular dispersion correction schemes include Grimme’s D3<sup>15,16</sup> and D4<sup>17–20</sup> corrections, different variants of Vydrov and van Voorhis’s VV10 model,<sup>21–23</sup> the exchange-hole dipole moment (XDM) model of Becke and Johnson,<sup>24–27</sup> or the Tkatchenko–Scheffler (TS) method.<sup>28,29</sup> Specifically, the efficient DFT-D approach has proven reliable in countless quantum chemical applications and workflows.<sup>30–33</sup>

Even though both spin-component-scaled (SCS) MP2 and spin-opposite-scaled (SOS) MP2 provide a reasonable result within short and medium ranges, they fail to correctly describe the long-range correlation. To address this issue, Lochan, Jung, and Head-Gordon proposed a distance-dependent mod-

<sup>a)</sup>these authors contributed equally

ification, where they split the electron interaction operator ( $1/r_{12}$ ) of SOS-MP2 into a short and a long-range part.<sup>34</sup> In the short-range regime, the MP2 energy is scaled by the usual factor SOS-MP2 of 1.3, but the long-range scaling factor is adjusted to 2.0 – which recovers the asymptotic MP2 interaction energy of distant fragments. This modified opposite-spin MP2 (MOS-MP2) has been shown to provide a significant improvement over SOS-MP2 for a variety of chemical problems involving both short-range and long-range interactions.<sup>34</sup> In this work of Lochan, Jung, and Head-Gordon, it was already mentioned, that an extension to the double-hybrid scheme could benefit the insufficient description of long-range dispersion in double-hybrid density functional theory.

The main objective of the present study is to demonstrate that an extension of the double-hybrid scheme to MOS-MP2 is possible and delivers good performance to possibly promote further developments in this field. Moreover, we shall investigate whether the modified opposite-spin-scaled double hybrids outperform their corresponding SOS-MP2-based counterparts when empirical dispersion correction is added.

## II. THEORY

### A. MOS-MP2

It is well known that SOS-MP2 systematically underestimates long-range correlation interactions. This can be accounted for by making the scaling factor distance-dependent, resulting in a range-separation analogous to range-separation in Hartree–Fock exchange, but for the MP2 correlation part.<sup>34</sup> The exchange operator in the MP2 integrals is replaced by the MOS operator

$$\widehat{g}_\omega(\mathbf{r}) = \frac{1}{\mathbf{r}} + c_{\text{MOS}} \frac{\text{erf}(\omega \mathbf{r})}{\mathbf{r}}, \quad (1)$$

where  $\omega$  determines the strength of attenuation. It leads to the modified integral

$$\tilde{I}_{ia}^{jb} = \int d\mathbf{r}' \phi_i(\mathbf{r}) \phi_a(\mathbf{r}) \widehat{g}_\omega(\mathbf{r} - \mathbf{r}') \phi_j(\mathbf{r}') \phi_b(\mathbf{r}'); \quad (2)$$

which provides the following energy expression for MOS-MP2

$$E_{\text{MP2}}^{\text{MOS}} = - \sum_{ia}^{\alpha} \sum_{jb}^{\beta} \frac{\tilde{I}_{ia}^{jb}(\omega) \tilde{I}_{ia}^{jb}(\omega)}{[\epsilon_a + \epsilon_b - \epsilon_i - \epsilon_j]}, \quad (3)$$

where  $i, j$  are the occupied and  $a, b$  are the virtual orbitals with corresponding eigenvalues,  $\epsilon$ . The MOS operator,  $\widehat{g}_\omega(\mathbf{r})$ , (Eq. 1) depends on two parameters,  $\omega$  and  $c_{\text{MOS}}$ .  $c_{\text{MOS}}$  can be fixed at  $\sqrt{2} - 1$  by using the condition of

$$\lim_{\mathbf{r} \rightarrow \infty} E_{\text{MP2}}^{\text{MOS}} = 2E_{\text{MP2}}^{\text{OS}}. \quad (4)$$

Hence, our MOS-MP2 scheme depends only on a single parameter,  $\omega$ . For main group chemistry problems, the Lochan, Jung, and Head-Gordon recommends  $\omega = 0.6$ . Similar to

SOS-MP2,<sup>35</sup> for MOS-MP2, the scaling factor for the same-spin MP2 correlation energy components is 0, but the parameter for the opposite-spin MP2 correlation ranges from 1.3 to 2.0.

### B. Double Hybrids: Hartree–Fock and MP2 Admixture

In 2006, Grimme proposed the so-called *double hybrid* functionals by combining a fraction of exact exchange and nonlocal GLPT2<sup>37</sup> (second-order Görling–Levy perturbation theory) correlation with the semilocal DFT exchange and correlation components.<sup>36</sup> These functionals have the following expression for the exchange-correlation energy

$$E_{XC}^{\text{DH}} = a_X E_X^{\text{HF}} + (1 - a_X) E_X^{\text{DFA}} + (1 - a_C) E_C^{\text{DFA}} + a_C E_C^{\text{MP2}}, \quad (5)$$

where  $E_X^{\text{DFA}}$  and  $E_C^{\text{DFA}}$  represent the semilocal exchange and correlation energy components;  $E_X^{\text{HF}}$  and  $E_C^{\text{MP2}}$  are the HF-exchange and GLPT2 correlation energies –  $a_X$  and  $a_C$  are the respective parameters. Previously, the term *gDH* was used for these types of functionals.<sup>38</sup> Later, Martin and coworkers showed that using separate parameters for the same and opposite-spin MP2 correlation (i.e.,  $a_{OS}$  and  $a_{SS}$ ) improved the accuracy of DHs for main-group thermochemistry and harmonic frequencies.<sup>39–44</sup>

Another family of double hybrids, which are often referred to as xDHs, uses full semilocal correlation instead for the generation of KS reference orbitals.<sup>38,45,46</sup> It was argued that such orbitals are more appropriate as a basis for GLPT2 than the damped-correlation orbitals in the gDHs.<sup>47,48</sup> However, this argument has been refuted on empirical grounds by Goerigk and Grimme and by Kesharwani, Kozuch, and Martin.<sup>45,49</sup> The XYG-family of double hybrids from Zhang, Xu, and Goddard, the xDSD(xDOD) and the XYG8 functionals by Santra, Semidalas, and Martin belong to this category.<sup>38,45–48,50–53</sup>

The exchange-correlation energy for a modified opposite-spin scaled double hybrid (MOS-DH) functional is expressed as

$$E_{XC}^{\text{MOS-DH}} = a_X E_X^{\text{HF}} + (1 - a_X) E_X^{\text{DFA}} + a_{C,\text{DFA}} E_C^{\text{DFA}} + a_{OS} E_C^{\text{MOS-MP2}}, \quad (6)$$

where  $E_X^{\text{DFA}}$ ,  $E_X^{\text{HF}}$ , and  $E_C^{\text{DFA}}$  represent the same energy component as in Eq. (5).  $a_X$  and  $a_{C,\text{DFA}}$  are the parameters for the HF-exchange and the semilocal-correlation energy components.  $E_C^{\text{MOS-MP2}}$  is the MOS-MP2 correlation energy component, and  $a_{OS}$  is the corresponding parameter. We refer to these new functionals as  $\text{MOS}_n\text{-XC}$  in the remaining text, where XC is a combination of DFA exchange and correlation and  $n$  is the percentage of HF-exchange (i.e.,  $n = 100a_X$ ). In passing, we must note that  $a_{C,\text{DFA}}$  in Eq. (6) and  $(1 - a_C)$  in Eq. (5) are the same parameters.

On the other hand, for the modified opposite-spin scaled version of the XYG8-family functional, the exchange-

correlation energy expression is

$$E_{XC}^{\text{MOS-XYG@BmLYP}} = a_X E_X^{\text{HF}} + a_{X,\text{DFA}} E_X^{\text{B88}} + a_{X,S} E_X^{\text{Slater}} + a_{C,\text{LDA}} E_C^{\text{VWN5}} + a_{C,\text{DFA}} E_C^{\text{LYP}} + a_{OS} E_C^{\text{MOS-MP2}}, \quad (7)$$

where  $E_X^{\text{HF}}$ ,  $E_C^{\text{MOS-MP2}}$ ,  $a_X$ , and  $a_{OS}$  represent the same as in Eq. (6);  $E_X^{\text{B88}}$  and  $E_X^{\text{Slater}}$  are the exchange energy components from the Becke88 generalized gradient approximation (GGA) and Slater-type local density approximation (LDA);  $a_{X,\text{DFA}}$  and  $a_{X,S}$  are corresponding parameters, respectively. The semilocal GGA and LDA correlation energies are represented by  $E_C^{\text{LYP}}$  and  $E_C^{\text{VWN5}}$ , where  $a_{C,\text{DFA}}$  and  $a_{C,\text{LDA}}$  are the respective coefficients for those energy components. The reference orbitals used in MOS-XYG are BmLYP [i.e.,  $m\%$  HFx + (100 -  $m$ )% DFTx + 19% VWN5 + 81% LYP]. We employed the same GGA-type and LDA-type exchange and correlation during the orbital generation as well as the final energy evaluation step.

### C. DFT-D4 Dispersion Correction

The default atomic-charge dependent D4 dispersion correction including Axilrod-Teller-Muto<sup>54,55</sup> (ATM) type three-body contributions was applied according to Eq. (8) with atomic indices  $A$ ,  $B$ , and  $C$ , their distance  $R_{AB}$ , the  $n^{\text{th}}$  dispersion coefficient  $C_{(n)}^{AB}$ , and the angle-dependent term  $\theta_{ABC}$

$$E_{disp}^{\text{D4}} = -\frac{1}{2} \sum_{AB} \sum_{n=6,8} s_n \frac{C_{(n)}^{AB}}{R_{AB}^{(n)}} f_{damp}^{(n)}(R_{AB}) \quad (8a)$$

$$-\frac{1}{6} \sum_{ABC} s_9 \frac{C_{(9)}^{ABC}}{R_{ABC}^{(9)}} f_{damp}^{(9)}(R_{ABC}, \theta_{ABC}) \quad (8b)$$

where  $f_{BJ}^{(n)}(R_{AB})$  corresponds to the default Becke-Johnson (BJ) damping function<sup>16</sup> according to Eq. (9):

$$f_{BJ}^{(n)}(R_{AB}) = \frac{R_{AB}^{(n)}}{R_{AB}^{(n)} + (a_1 R_0^{AB} + a_2)^{(n)}}. \quad (9)$$

The usually fitted parameters for a non-DH functional are  $s_8$ ,  $a_1$ , and  $a_2$ . For a DH,  $s_6$  must also be adjusted due to the presence of the MP2 correlation term. As in Refs. 14,38,53, the parameter controlling the three-body contribution was set to  $s_9 = 1$  for all MOS-MP2-based double hybrids.

### III. COMPUTATIONAL DETAILS

Unless otherwise specified, all calculations were performed using the Q-Chem 5.4 quantum chemistry program package.<sup>56</sup> The Weigend-Ahlrichs quadruple- $\zeta$  basis set def2-QZVPP<sup>57</sup> was used for all calculations. For seven GMTKN55 subsets (WATER27,<sup>58</sup> RG18,<sup>59</sup> IL16,<sup>60</sup> G21EA,<sup>61</sup> AHB21,<sup>60</sup>

BH76,<sup>62-64</sup> and BH76RC<sup>64</sup>) the diffuse-function-augmented def2-QZVPPD<sup>65</sup> was employed instead. The matching effective core potentials (ECPs)<sup>66,67</sup> for heavy elements with  $Z > 36$  were generally employed. For the MP2 part, RI approximation was applied to accelerate the calculations in conjunction with the def2-QZVPPD-RI<sup>68,69</sup> auxiliary basis set. The SG-3<sup>70</sup> integration grid was employed, except for the SCAN (strongly constrained and appropriately normed) variants,<sup>71</sup> where an unpruned (150, 590) grid was used for its severe integration grid sensitivity.<sup>72</sup> Similar to Ref. 46, for the SCF energy components of MOS-XYG double hybrids, the MRCC2020 package was used.<sup>73</sup>

DFT-D4 dispersion corrections were calculated with the `df-t-d4 3.4.0` standalone program.<sup>17-20</sup>

Reference geometries for the GMTKN55 benchmark sets were taken from Ref. 59. Additionally, the transition-metal chemistry sets CUAGAU-2,<sup>74</sup> LTMBH,<sup>75</sup> MOBH35,<sup>76-78</sup> MOR41,<sup>79</sup> ROST61,<sup>80</sup> TMBH,<sup>81-84</sup> TMCONF16,<sup>85</sup> TMIP,<sup>86</sup> and WCCR10<sup>87,88</sup> are evaluated – this compilation of benchmark sets will be referred to as *TM* throughout this document.

### IV. PARAMETRIZATION STRATEGY

The modified opposite-spin scaled double hybrid functionals have been parameterized using the GMTKN55 benchmark suite.<sup>59</sup> This dataset consists of 55 types of chemical problems, which can be further divided into five subsets: basic thermochemistry of small molecules, barrier heights, large molecule reactions, intermolecular interactions, and conformer energies.

Originally proposed by Goerigk *et al.*, the WTMAD-2<sup>59</sup> (weighted total mean absolute deviation) has been used as the primary metric for the performance evaluation and parameter optimization of the MOS-DHs. From a statistical viewpoint, MAD (mean absolute deviation) is a more robust metric than RMSD (root-mean-square deviation), as the former is more resilient to a small number of large outliers than the latter.<sup>89</sup> For a normal distribution without a systematic error, RMSD  $\approx \frac{5}{4}$  MAD.<sup>90</sup> See Appendix B in the Supporting Information for the definition of the used statistical measures.

The constructed MOS-DH functionals have four empirical parameters:

- (a) fraction of exact exchange ( $a_X$ )
- (b) fraction of the semilocal DFT correlation ( $a_{C,\text{DFA}}$ )
- (c) coefficient for the MOS-MP2 correlation ( $a_{OS}$ )
- (d) parameter  $\omega$  controls the level of attenuation of the MOS operator

The MOS-XYG double hybrid scheme contains three additional parameters:

- (e) fraction of B88 exchange ( $a_{X,\text{DFA}}$ )
- (f) fraction of Slater exchange ( $a_{X,S}$ )
- (g) fraction of local correlation ( $a_{C,\text{LDA}}$ )

Powell’s BOBYQA (bound optimization by quadratic approximation) derivative-free constrained optimizer was used for the optimization.<sup>91</sup> For a given set of  $\{a_X, a_{C,DFA}, \omega\}$ , it is possible to obtain the optimal value of  $a_{OS}$  without any further electronic structure calculations simply by extracting individual energy components from the calculations, evaluating total energies and hence WTAD-2 for a given  $a_{OS}$ , and minimizing WTAD-2 with respect to  $a_{OS}$  using BOBYQA. It can be considered as the *microiteration* loop. In comparison, the outer *macroiteration* loop consists of varying  $\{a_X, a_{C,DFA}, \omega\}$  and reevaluating the full GMTKN55 using the updated set of parameters. For the revised DSD and DOD functionals, we found that  $a_{C,DFA}$  could be safely included in the microiteration, but  $a_X$  could not due to its strong coupling with the MP2 scaling factors.<sup>43</sup> Hence, we have adopted the practice of microiterating  $\{a_{C,DFA}, a_{OS}\}$  at every macroiteration using BOBYQA. We must note that, with full microiteration cycles, additional macroiterations beyond the first typically do not have significantly improved performance unless the starting guess is especially poor. Hence, the output of the first cycle is reported. The optimum value of  $\omega$  for each  $a_X$  was determined manually by interpolation.

For each exchange-correlation combination, the above-mentioned process is repeated with multiple  $a_X$  values to find the best MOS-DH, which offers the lowest WTAD-2.

While using D4 dispersion correction with MOS-DHs, four extra parameters needed to be included in the microiteration loop:  $s_6, s_8, s_9, a_1,$  and  $a_2$ . Hence, for each  $\{a_X, \omega\}$  set, we optimized  $\{a_{C,DFA}, a_{OS}, s_6, s_8, s_9, a_1, a_2\}$ . Like in revDSD-PBEP86-D4 and xDSD<sub>75</sub>-PBEP86-D4, the  $s_9 = 1$  constraint was used across the board while optimizing the other microiteration parameters of MOS-DH-D4 functionals.

For optimizing the MOS-XYG parameters, the same protocol as in Ref. 46 was used. Except for  $\omega$ , all the parameters were included in the microiteration loop. For the *BmLYP* reference orbitals, the value of  $m$  has been optimized manually by interpolation.

## V. RESULTS AND DISCUSSION

### A. Main Group Chemistry Problems (GMTKN55)

To evaluate the impact of using MOS-MP2 as the nonlocal correlation part of double hybrids, the SOS-MP2 components of noDispOD<sub>69</sub>-PBEP86 and xnoDispOD<sub>72</sub>-PBEP86 are replaced with MOS-MP2, and the corresponding parameters are reoptimized, keeping the other parameters unchanged. As a result, the WTAD-2<sub>GMTKN55</sub> values improved by 1.25 and 1.17 kcal·mol<sup>-1</sup> for their respective MOS-MP2-based counterparts. For both cases, the lion’s share of this improvement comes from basic thermochemistry and the two non-covalent interaction subsets (Fig. 1). Especially the W4-11,<sup>92</sup> PCONF21,<sup>93,94</sup> and S66<sup>95</sup> subsets of the GMTKN55 improved significantly. Because MOS-MP2 uses a distance-dependent scaling factor (ranging from 1.3 to 2.0), the optimized  $a_{OS}$  for the MOS-MP2-based double hybrid is smaller than its SOS-MP2-based counterpart noDispOD<sub>69</sub>-PBEP86.

The ratio of  $a_{OS}$  between SOS-MP2 and MOS-MP2-based double hybrids is 1.4, which increases to 1.7 with the increase of  $a_X$  from 0.69 to 0.82 (Tab. S2 in the Supporting Information).

Using MOS-MP2 instead of SOS-MP2 greatly enhances the accuracy of dispersion-uncorrected double hybrids, prompting us to optimize all parameters of MOS-DH functionals further. The final parameters and WTAD-2<sub>GMTKN55</sub> values for the GMTKN55 for various MOS-DHs and their corresponding SCS-MP2-based dispersion-free counterparts are listed in Tab. I.

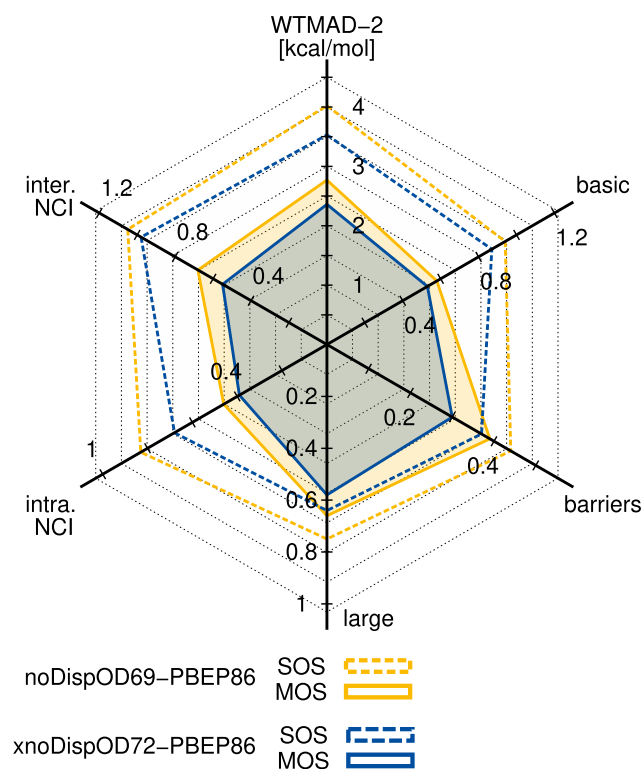


FIG. 1. Effect of using MOS-MP2 in a double hybrid functional on total WTAD-2<sub>GMTKN55</sub> and  $\Delta$ WTAD-2 contributions from five major subsets of GMTKN55. The numbers are given in kcal·mol<sup>-1</sup>.

While using the PBE-P86 exchange-correlation combination, varying the percentage of HF-exchange and the MOS-MP2 range-separation parameter ( $\omega$ ) simultaneously, we obtained the lowest WTAD-2<sub>GMTKN55</sub> of 2.48 kcal·mol<sup>-1</sup> with  $a_X = 0.76$  and  $\omega = 0.50$  (Fig. 2 and Tab. I). Among the five major subcategories of the GMTKN55, barrier heights and non-covalent interactions benefit the most upon using MOS-MP2 (see Tab. II). The major share of this improvement comes from the BH76,<sup>62-64</sup> S66,<sup>95</sup> RSE43,<sup>96</sup> and PCONF21<sup>93,94</sup> subsets. On the other hand, the performance on, e.g., the bond-separation reactions of saturated hydrocarbons subset BSR36 is worsened.<sup>97,98</sup> When compared to the revDOD-PBEP86-D4, the absence of empirical dispersion correction significantly deteriorates the accuracy of MOS<sub>76</sub>-PBEP86 for the pericyclic reaction barrier heights,<sup>64,99-101</sup> BH76,<sup>62-64</sup> RSE43,<sup>96</sup> and RG18<sup>59</sup> subsets, but outperforms

TABLE I. Final parameters and total WTMAD-2<sub>GMTKN55</sub> of the MOS-DHs and their respective spin-component-scaled, dispersion uncorrected DHs on the GMTKN55 in kcal·mol<sup>-1</sup>.

Functional	WTMAD-2	$\omega$	$a_X$	$a_{X,DFA}$	$a_{X,S}$	$a_{C,DFA}$	$a_{C,LDA}$	$a_{OS}$	$a_{SS}$
MOS <sub>76</sub> -PBEP86	2.48	0.5000	0.7600	0.2400	—	0.4371	—	0.5602	[0]
xMOS <sub>78</sub> -PBEP86	2.27	0.6500	0.7800	0.2200	—	0.4056	—	0.5373	[0]
MOS-XYG@B <sub>50</sub> LYP	2.05	0.9000	0.8871	-0.1087	0.2165	[0]	0.3982	0.4406	[0]
noDispSD <sub>82</sub> -PBEP86	2.89	—	0.8200	0.1800	—	0.3073	—	0.7426	0.3782
xnoDispSD <sub>82</sub> -PBEP86	2.51	—	0.8200	0.1800	—	0.2797	—	0.7678	0.3521
XYG8[f <sub>2</sub> ]@B <sub>25</sub> LYP <sup>46</sup>	1.92	—	0.9144	-0.1537	0.2132	[0]	0.4928	0.4540	0.2780

revDOD-PBEP86-D4 for the tautomer relative energies.

For a specific MOS-MP2 range-separation parameter  $\omega$ , an increasing percentage of HF-exchange yields a larger optimized value of the MOS-MP2 correlation parameter  $a_{OS}$ , while the fraction of the semilocal DFT correlation decreases (Fig. 3). On the other hand, for a fixed value of  $a_X$ , increasing  $\omega$  yields a lower  $a_{OS}$ . For a very small  $\omega$  (i.e.,  $\omega < 0.5$ )  $a_{C,DFA}$  decreases (Tab. S9 in the Supporting Information). The trend of the WTMAD-2<sub>GMTKN55</sub> against the optimized  $a_{OS}$  is shown in Fig. S2 in the Supporting Information.

For the revDSD- and revDOD-family double hybrids, we achieved the lowest WTMAD-2<sub>GMTKN55</sub> using only the PBE-P86 exchange-correlation combination, as noted by Santra, Sylvetsky, and Martin. Until now, we have only used the PBE exchange and P86 correlation. Similarly, however, for the MOS-DHs, using the SCAN-SCAN and PBE-PBE exchange-correlation combinations resulted in worse performance compared to their PBE-P86-based counterparts. Among the PBE-based functionals, the lowest WTMAD-2<sub>GMTKN55</sub> was obtained with  $a_X = 0.78$  and  $\omega = 0.50$ . On the other hand, for the MOS<sub>n</sub>-SCAN type functionals, the optimum values of the parameters are 0.74 and 0.90, respectively (Tab. S2 and Fig. S1 in the Supporting Information). For each  $\{a_X, \omega\}$  combination, the WTMAD-2<sub>GMTKN55</sub> error statistics for the SCAN- and PBE-based MOS-DHs are listed in TABLES S6 and S7 in the Supporting Information, respectively.

For the xDH variant, we obtained the lowest WTMAD-2<sub>GMTKN55</sub> of 2.27 kcal·mol<sup>-1</sup> by employing  $a_X = 0.78$  and  $\omega = 0.65$  (Fig. 2). The improvement in WTMAD-2<sub>GMTKN55</sub> for the MOS-type double hybrid is 0.21, whereas, for the noDispSD functionals, that improvement is 0.37 kcal·mol<sup>-1</sup> (Tab. I). The majority of that improvement for MOS-DHs originates from the large-species reaction energies. Further inspection reveals that for the RSE43 set, the performance of xMOS<sub>78</sub>-PBEP86 is noticeably better than MOS<sub>76</sub>-PBEP86. For a fixed value of  $\omega$ , an increasing amount of HF exchange also leads to a larger optimal value of  $a_{OS}$  and simultaneously smaller  $a_{C,DFA}$  (Fig. 3 and Tab. S10 in the Supporting Information). The performance comparison with optimized  $a_{OS}$  is given in Fig. S2 in the Supporting Information.

Comparing the performance of xMOS<sub>78</sub>-PBEP86 and xnoDispSD<sub>82</sub>-PBEP86, we found that the barrier heights, inter- and intramolecular non-covalent interactions benefit from MOS-MP2 over SCS-MP2. Although for most of the re-

action types of GMTKN55, xMOS<sub>78</sub>-PBEP86 performs better than xnoDispSD<sub>82</sub>-PBEP86, for small molecule atomization energies (W4-11), decomposition energies of a few artificial molecules (MB16-43), and bond-separation reactions of saturated hydrocarbons (BSR36), xnoDispSD<sub>82</sub>-PBEP86 outperforms by a significant margin.

Interestingly enough, the WTMAD-2<sub>GMTKN55</sub> gap between xMOS<sub>78</sub>-PBEP86 and xDOD<sub>72</sub>-PBEP86-D4 is only 0.07 kcal·mol<sup>-1</sup>. Except for the basic thermochemistry and intramolecular interactions, xDOD<sub>72</sub>-PBEP86-D4 outperforms xMOS<sub>78</sub>-PBEP86 for the remaining three GMTKN55 subsets (Tab. II and Tab. S3 in the Supporting Information).

For a fixed value of  $a_X$ , the remaining parameters of xMOS<sub>n</sub>-PBEP86 and xDOD<sub>n</sub>-PBEP86-D4 are optimized and their performance is evaluated. It is clear that the WTMAD-2<sub>GMTKN55</sub> gap decreases gradually from  $a_X = 0.50$  to  $a_X = 0.78$ . Beyond 78% HF-exchange, MOS-DHs outperform the respective SOS-MP2-based dispersion corrected xDHs (Fig. 4 and Tab. S13 in the Supporting Information). Only for the basic thermochemistry reactions, xMOS-DHs are better than the respective xDOD-D4 functionals, and performance difference increases with the increasing amount of Hartree-Fock exchange (Fig. 4). For the remaining four reaction types of the GMTKN55, the xDOD-D4 functionals outperform the xMOS-DHs for a small percentage of HF-exchange. On the other hand, at larger percentages (e.g.,  $a_X = 0.85$ ), xMOS-DH offers better performance for barriers compared to the corresponding xDOD-D4. For inter- and intramolecular non-covalent interactions, both double hybrid schemes offer similar accuracy (Fig. S3 in the Supporting Information). The optimized parameters of xMOS<sub>n</sub>-PBEP86 and xDOD<sub>n</sub>-PBEP86-D4 can be found in TABLES S11 and S12 in the Supporting Information.

An increasing amount of Hartree-Fock admixture leads to a decreasing difference in overall main-group performance between xMOS<sub>n</sub>-PBEP86 and xnoDispOD<sub>n</sub>-PBEP86. For basic thermochemistry reactions, the difference between xMOS<sub>50</sub>-PBEP86 and xnoDispOD<sub>50</sub>-PBEP86 is small, but increases at larger percentages of HF-exchange (Fig. 4). On the other hand, for the remaining four subsets, the  $\Delta$ WTMAD-2 difference gradually decreases with the increase in  $a_X$  (Fig. S3 in the Supporting Information).

In a recent study, Martin and co-workers reported that using an elevated percentage of HF-exchange and separate param-

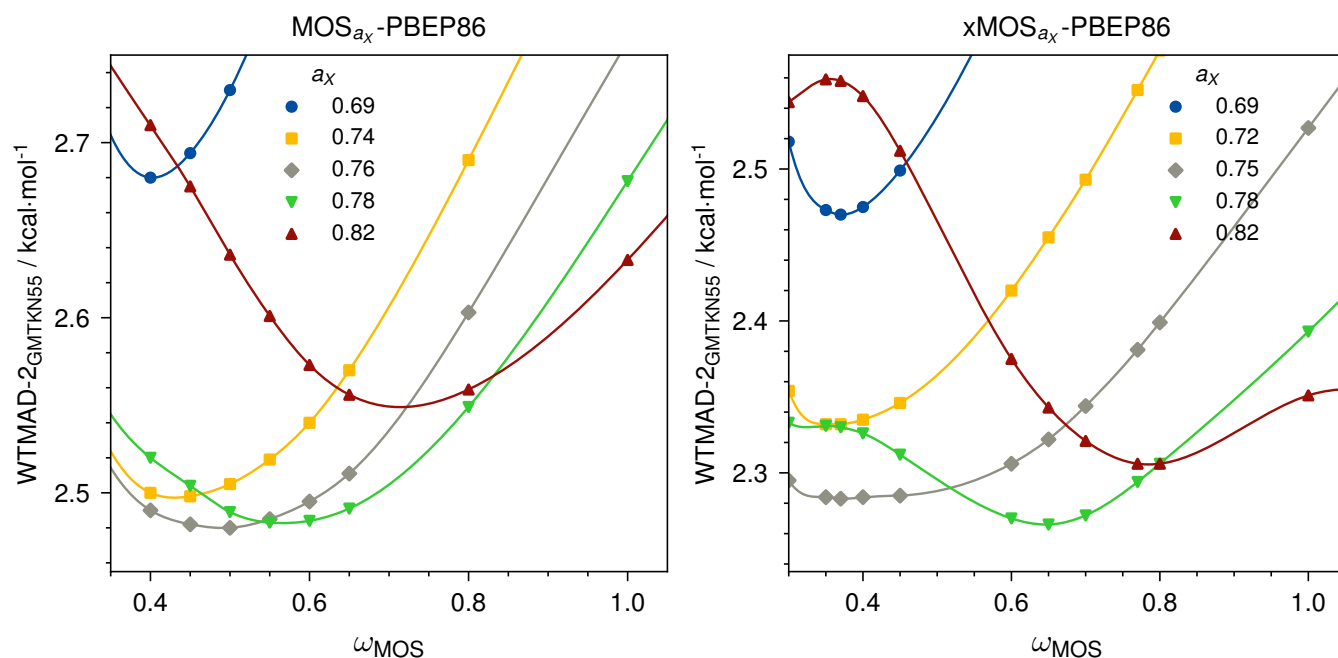


FIG. 2. Dependence of WTMAD-2<sub>GMTPKN55</sub> (kcal·mol<sup>-1</sup>) on the MOS-MP2 range-separation parameter  $\omega$  for MOS<sub>a<sub>x</sub></sub>-PBEP86 and xMOS<sub>a<sub>x</sub></sub>-PBEP86.

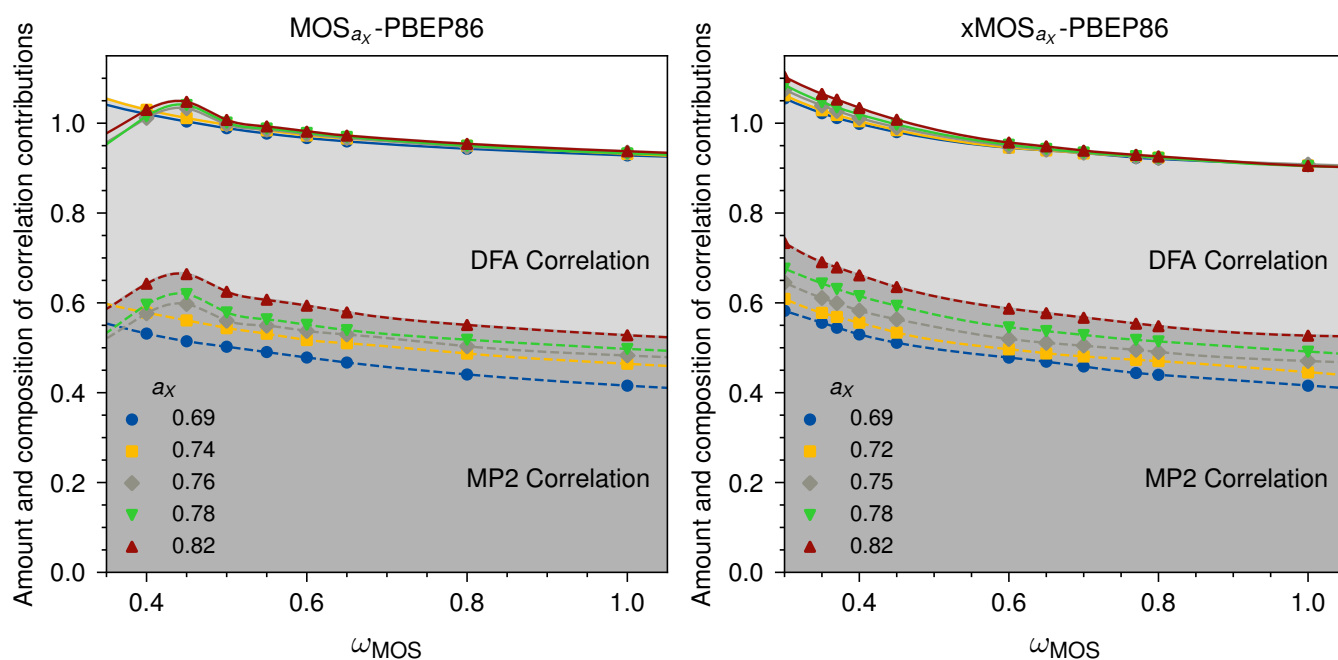


FIG. 3. Dependence of the optimised amounts of MOS-MP2 and DFA correlation on the MOS-MP2 range-separation parameter  $\omega$  for MOS<sub>a<sub>x</sub></sub>-PBEP86 and xMOS<sub>a<sub>x</sub></sub>-PBEP86.

ters for the local and semilocal exchange and correlation energy components, XYG8[ $f_2$ ]<sub>B<sub>25</sub>LYP</sub> offered very good performance (WTMAD-2 of 1.92 kcal·mol<sup>-1</sup>) without employing any empirical dispersion correction.<sup>46</sup> While other dispersion uncorrected double hybrids listed in Table I have only 4 empirical parameters, XYG8[ $f_2$ ]<sub>B<sub>25</sub>LYP</sub> contains 6.

For the MOS-XYG@*Bm*LYP functional, six different types of orbitals were tested, with the percentage of HF-exchange varying from 10% to 70%, and for each reference orbital, MOS-MP2 correlation was evaluated with seven different  $\omega$  values (Tab. S7 in the Supporting Information). Among the modified SOS-MP2 double hybrids reported in the

TABLE II. WTMAD-2 and the  $\Delta$ WTMAD-2 contributions of the five major subsets to total WTMAD-2<sub>GMTKN55</sub> in kcal·mol<sup>-1</sup>.

Functional	WTMAD2	basic	barrier	large	intra. NCI	inter. NCI
MOS <sub>76</sub> -PBEP86	2.48	0.52	0.37	0.64	0.41	0.55
xMOS <sub>78</sub> -PBEP86	2.27	0.52	0.32	0.54	0.38	0.51
MOS-XYG@B <sub>50</sub> LYP	2.05	0.52	0.29	0.43	0.37	0.44
noDispSD <sub>82</sub> -PBEP86	2.89	0.57	0.49	0.65	0.51	0.66
xnoDispSD <sub>82</sub> -PBEP86	2.51	0.52	0.40	0.53	0.46	0.61
XYG8[ <i>f</i> <sub>2</sub> ]@B <sub>25</sub> LYP <sup>46</sup>	1.92	0.46	0.23	0.36	0.43	0.44
revDOD-PBEP86-D4 <sup>38</sup>	2.27	0.58	0.25	0.58	0.40	0.46
xDOD <sub>72</sub> -PBEP86-D4 <sup>38,53</sup>	2.20	0.57	0.23	0.51	0.41	0.47
Pr <sup>2</sup> SCAN69-D4 <sup>14</sup>	2.72 <sup>(a)</sup>	0.62	0.36	0.58	0.59	0.56

<sup>(a)</sup>Due to the use of def2-QZVPPD basis set for seven GMTKN55 subsets (WATER27, RG18, IL16, G21EA, AHB21, BH76, and BH76RC) in the present work, the total WTMAD-2<sub>GMTKN55</sub> is 0.09 kcal/mol lower than what is reported in Ref. 14

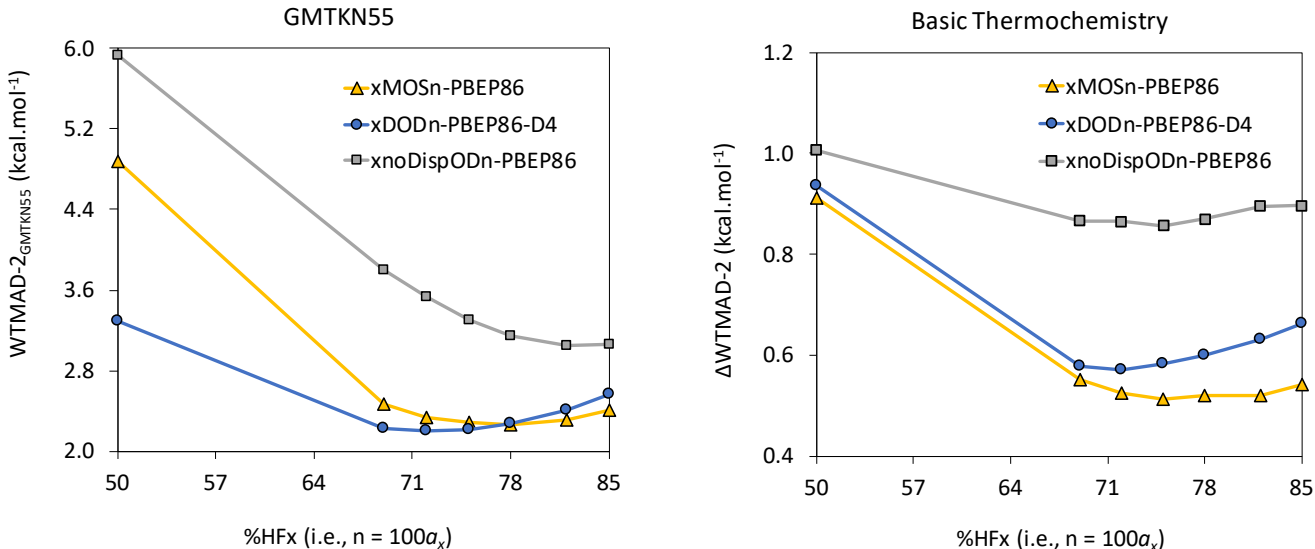


FIG. 4. Dependence of total WTMAD-2<sub>GMTKN55</sub> and  $\Delta$ WTMAD-2 for the basic thermochemistry reactions of GMTKN55 on different percentages of HF-exchange (i.e.,  $n = 100a_x$ ) in xMOS<sub>n</sub>-PBEP86, xnoDispSD<sub>n</sub>-PBEP86, and xDOD<sub>n</sub>-PBEP86-D4.

present study, MOS-XYG@B<sub>50</sub>LYP has the lowest WTMAD-2<sub>GMTKN55</sub> of 2.05 kcal·mol<sup>-1</sup>. Similar to the XYG8 functionals, for MOS-XYG, the optimized value of  $a_{C,DFA}$  is found to be nearly zero; fixing  $a_{C,DFA} = 0$  during optimization does not influence the overall performance.

Unlike the previous cases, for the XYG family functionals, WTMAD-2<sub>GMTKN55</sub> for the MOS-MP2-based double hybrid is 0.13 kcal·mol<sup>-1</sup> higher than its SCS-MP2-based counterpart (Tab. I). Comparing the WTMAD-2<sub>GMTKN55</sub> contributions from Tab. II, it is evident that the deterioration in the performance of MOS-XYG@B<sub>50</sub>LYP comes from the basic thermochemistry, barrier heights, and large molecule reaction energies. Upon further inspection, the main cause of the decrease in performance is due to the BH76 and BSR36 subsets. It is interesting to note that the MOS-MP2 XYG-family double hybrid, MOS-XYG@B<sub>50</sub>LYP, performs marginally bet-

ter than the dispersion-corrected SOS-MP2-based functional, XYG8[*f*<sub>2,os</sub>]@B<sub>30</sub>LYP. For the TAUT15, BSR36, and BHPER subsets, the MOS-XYG double hybrid offers better performance than XYG8[*f*<sub>2,os</sub>]@B<sub>30</sub>LYP, but for the BH76, W4-11, BH76RC, and RSE43<sup>96</sup> reactions, XYG8[*f*<sub>2,os</sub>]@B<sub>30</sub>LYP is superior.

## B. Effect Dispersion Correction

For this purpose, we use MOS<sub>n</sub>-PBEP86 and xMOS<sub>n</sub>-PBEP86 series and combine them with the DFT-D4 dispersion correction. Contrary to Refs. 38,43, the optimized  $s_8$  parameters of MOS<sub>n</sub>-PBEP86 are not always close to zero. For a specific percentage of HF exchange, that parameter only vanishes for small  $\omega$  values. With D4 dispersion cor-

rection, the lowest  $\text{WTMAD-2}_{\text{GMTKN55GMTKN55}}$  was obtained with  $a_X = 0.69$  and  $\omega = 0.10$ . The  $\text{WTMAD-2}_{\text{GMTKN55S}}$  listed in Table S13 indicate that the performance of MOS-PBEP86-D4 is approaching the limit of revDOD-PBEP86-D4. Conversely, the performance of  $\text{xMOS}_n\text{-PBEP86-D4}$  is somewhat heterogeneous, exhibiting both advantages and disadvantages (Tab. S14 in the Supporting Information). The optimized  $\text{WTMAD-2}_{\text{GMTKN55}}$  of  $\text{xMOS}_{72}\text{-PBEP86-D4}$  ( $\omega = 0.2$ ) is very close to the  $\text{xDOD}_{72}\text{-PBEP86-D4}$ . Hence, for the GMTKN55 reactions, the D4 dispersion-corrected MOS double hybrids are not better than revDOD-PBEP86-D4 and  $\text{xDOD}_{72}\text{-PBEP86-D4}$ . When dispersion-corrected and uncorrected  $\text{MOS}_{76}\text{-PBEP86}$  ( $\omega = 0.50$ ) and  $\text{xDOD}_{78}\text{-PBEP86}$  ( $\omega = 0.65$ ) correlation parameters are compared, it is found, that  $a_{OS}$  and  $a_{C,DFA}$  decrease slightly upon including D4 (Tab. S15 in the Supporting Information).

For the PBEP86, SCAN, and PBE-based MOS-double hybrids, the summation of the empirical  $a_{C,DFA}$  and  $a_{OS}$  are very close to unity. Setting the constraint of  $a_{C,DFA} + a_{OS} = 1.0$  during optimization, parameters and  $\text{WTMAD-2}_{\text{GMTKN55}}$  errors as shown in Tab. S12 in the Supporting Information are obtained. We find, that reducing the number of empirically fitted parameters from 4 to 3 has no noticeable influence on the performance of the tested MOS-DHs. The only exception is  $\text{MOS}_{78}\text{-PBE}$ , where the  $\text{WTMAD-2}_{\text{GMTKN55}}$  is increased by  $0.15 \text{ kcal}\cdot\text{mol}^{-1}$ . The majority of this performance loss comes from the intermolecular non-covalent interactions subset, most of which are due to the S66 non-covalent interactions set. During the optimization, the parameters  $a_X$  and  $\omega$  values for MOS-PBEP86 are found to be unchanged. For MOS-SCAN and MOS-PBE, only the optimized  $\omega$  value changed. On the other hand, for  $\text{xMOS}\text{-PBEP86}$ , both the  $a_X$  and  $\omega$  values deviate from the unconstrained optimization.

### C. Transition Metal Reactions

The mean absolute errors of the present functionals on the nine transition metal subsets with their respective total  $\text{WTMAD-2}_{\text{TM}}$  are presented in Tab. III and Tab. S23 in the Supporting Information.

For both,  $\text{MOS}_{76}\text{-PBEP86}$  and  $\text{xMOS}_{78}\text{-PBEP86}$  we find a very similar  $\text{WTMAD-2}_{\text{TM}}$  of 2.84 and 2.69  $\text{kcal}\cdot\text{mol}^{-1}$ , respectively. This is also reflected in the mean absolute errors of individual subsets.  $\text{MOS}_{76}\text{-PBEP86}$  is found to perform better on the ROST61 and WCCR10 sets, whereas  $\text{xMOS}_{78}\text{-PBEP86}$  performs better on the TMIP and CUAGAU-2.

A comparison of both MOS double-hybrids to revDSD-PBEP86-D4 or  $\text{Pr}^2\text{SCAN69-D4}$  reveals poor performance on nearly all transition-metal sets.<sup>14</sup> Of those sets, the barrier-height sets are the least affected, which is likely due to the large amounts of Hartree-Fock exchange. At the same time, this large amount is likely responsible for the deterioration of performance for the transition-metals. Large amounts of Fock-exchange can sometimes be favorable for main-group thermochemistry – as observed for GMTKN55 – but can potentially be problematic for transition-metal chemistry where a higher degree of static correlation effects can be expected.

Especially open-shell transition-metal complexes are prone to static correlation effects as found on the ROST61, CUAGAU-2, and TMIP.<sup>102</sup>

While  $\text{MOS-XYG@B}_{50}\text{LYP}$  showed excellent accuracy on the GMTKN55 for main-group thermochemistry, it is not transferable to our TM datasets. It has the highest  $\text{WTMAD-2}_{\text{TM}}$  of 5.23  $\text{kcal}\cdot\text{mol}^{-1}$  among all tested functionals.

Comparing the mean  $\text{WTMAD-2}$  values of GMTKN55 and TM datasets ( $\text{WTMAD-2}_{\text{Mean}}$ ), it is evident that  $\text{xMOS}_{78}\text{-PBEP86}$  is the best performer among the new MOS double hybrids. However, it still underperformed compared to regular SOS/SCS-MP2-based dispersion-corrected functionals, such as revDSD-PBEP86-D4 or  $\text{Pr}^2\text{SCAN69-D4}$  (Fig. 5).

## VI. CONCLUSIONS

We have proposed a new variety of double hybrid functionals using the modified opposite-spin MP2 as the nonlocal correlation component. From our investigation of MOS-DHs and their respective DOD- and DSD-family counterparts with the aid of the GMTKN55 and nine additional transition-metal data sets, we can conclude the following:

- (a) Except for the MOS-XYG functional, the MOS-MP2-based double hybrids always outperform their SCS-MP2-based counterparts on the GMTKN55 without the addition of any dispersion correction.
- (b) The major benefit of distance-dependent MP2 compared to regular MP2 in double hybrids originates from the poor description of long-range correlation effects, which is especially important for inter- and intramolecular non-covalent interactions.
- (c) For a fixed value of HF-exchange in MOS-DHs, gradually increasing attenuation parameter ( $\omega$ ) requires a systematically smaller amount of total MOS-MP2 correlation.
- (d) Among all the MOS-DHs tested in the present study, the six-parameter  $\text{MOS-XYG@B}_{50}\text{LYP}$  has the lowest  $\text{WTMAD-2}_{\text{GMTKN55}}$  of 2.05  $\text{kcal}\cdot\text{mol}^{-1}$ , but with a large percentage of HF-exchange and large a  $\omega$  MOS-MP2 attenuation parameter. However, for the transition-metal-involving reactions, it yields the worst  $\text{WTMAD-2}_{\text{TM}}$ .
- (e) The four-parameter  $\text{xMOS}_{78}\text{-PBEP86}$  shows the best overall performance, balancing main-group and transition-metal chemistry performance. However, in terms of the  $\text{WTMAD-2}_{\text{Mean}}$ , the dispersion uncorrected  $\text{xMOS}_{78}\text{-PBEP86}$  performs worse than  $\text{Pr}^2\text{SCAN69-D4}$  and revDSD-PBEP86-D4.
- (f) When D4 correction is incorporated into double hybrids, using the MOS-MP2 scheme does not provide additional benefits compared to simple SOS-MP2.



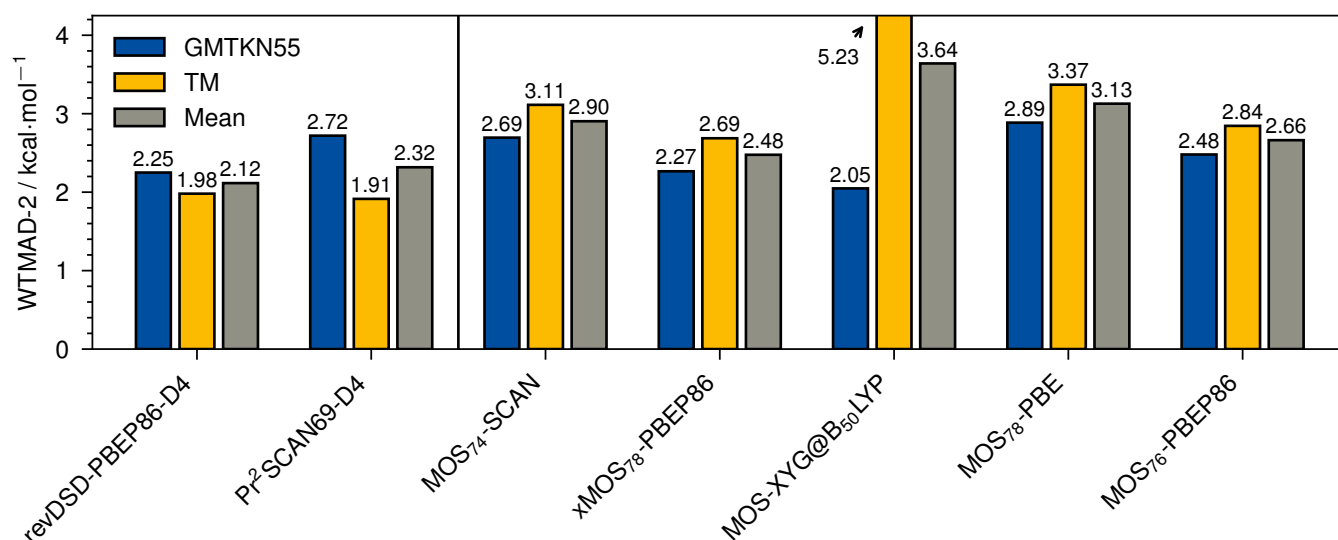


FIG. 5. WTMAD-2 error statistics for GMTKN55, the transition-metal sets, and their mean for selected MOS-double-hybrids, revDSD-PBEP86-D4, and Pr<sup>2</sup>SCAN69-D4. The results for revDSD-PBEP86-D4 and Pr<sup>2</sup>SCAN69-D4 are extracted from reference.<sup>14</sup>

TABLE III. WTMAD-2 and MAEs of metal-organic benchmark sets in kcal·mol<sup>-1</sup>. The revDSD-PBEP86-D4 and Pr<sup>2</sup>SCAN69-D4 error statistics are taken from reference.<sup>14</sup>

Functional	WTMAD-2 <sub>TM</sub>	CUAGAU-2	LTMBH	MOBH35	MOR41	ROST61	TMBH	TMCONF16	TMIP	WCCR10
MOS <sub>76</sub> -PBEP86	2.84	4.17	0.88	1.65	3.82	3.43	1.13	0.22	14.85	1.65
xMOS <sub>78</sub> -PBEP86	2.69	4.01	0.80	1.62	3.79	2.95	1.13	0.23	10.31	1.80
MOS-XYG@B <sub>50</sub> LYP	5.23	6.74	1.54	4.07	5.86	5.97	3.10	0.21	11.47	5.19
revDSD-PBEP86-D4 <sup>14,103</sup>	1.98	2.89	0.57	1.42	2.81	2.04	0.84	0.18	9.01	1.45
Pr <sup>2</sup> SCAN69-D4 <sup>14</sup>	1.91	3.23	0.40	1.62	2.40	1.96	0.98	0.16	7.96	1.86

## ACKNOWLEDGEMENT

G.S. thanks Prof. Jan M. L. Martin (Dept. of Molecular Chemistry and Materials Science, Weizmann Institute of Science, Rehovot, Israel) for kindly allowing access to the ChemFarm HPC cluster of the Weizmann Institute Faculty of Chemistry. All calculations for parameterizing the modified opposite-spin-scaled double-hybrid functionals were performed on ChemFarm.

L.W. greatly acknowledges the support of the Stiftung Stipendien-Fonds des Verbandes der Chemischen Industrie e.V. through its Kekulé Fellowship.

L.W. would like to extend his gratitude to Prof. Stefan Grimme for his exceptional support and for granting access to the computational resources at the Mulliken Center for Theoretical Chemistry.

## DATA AVAILABILITY STATEMENT

Raw data can be obtained upon reasonable request.

## REFERENCES

- <sup>1</sup>A. M. Teale, T. Helgaker, A. Savin, C. Adamo, B. Aradi, A. V. Arbuznikov, P. W. Ayers, E. J. Baerends, V. Barone, P. Calaminici, E. Cancès, E. A. Carter, P. K. Chattaraj, H. Chermette, I. Ciofini, T. D. Crawford, F. D. Proft, J. F. Dobson, C. Draxl, T. Frauenheim, E. Fromager, P. Fuentealba, L. Gagliardi, G. Galli, J. Gao, P. Geerlings, N. Gidopoulos, P. M. W. Gill, P. Gori-Giorgi, A. Görling, T. Gould, S. Grimme, O. Gritsenko, H. J. A. Jensen, E. R. Johnson, R. O. Jones, M. Kaupp, A. M. Köster, L. Kronik, A. I. Krylov, S. Kvaal, A. Laestadius, M. Levy, M. Lewin, S. Liu, P.-F. Loos, N. T. Maitra, F. Neese, J. P. Perdew, K. Pernal, P. Pernot, P. Piecuch, E. Rebolini, L. Reining, P. Romaniello, A. Ruzsinszky, D. R. Salahub, M. Scheffler, P. Schwerdtfeger, V. N. Staroverov, J. Sun, E. Tellgren, D. J. Tozer, S. B. Trickey, C. A. Ullrich, A. Vela, G. Vignale, T. A. Wesolowski, X. Xu, and W. Yang, "DFT exchange: sharing perspectives on the workhorse of quantum chemistry and materials science," *Phys. Chem. Chem. Phys.* **24**, 28700–28781 (2022).
- <sup>2</sup>M. Bursch, J.-M. Mewes, A. Hansen, and S. Grimme, "Best-Practice DFT Protocols for Basic Molecular Computational Chemistry," *Angew. Chemie* **134**, e202205735 (2022).
- <sup>3</sup>J. P. Perdew and K. Schmidt, "Jacob's ladder of density functional approximations for the exchange-correlation energy," *AIP Conf. Proc.* **577**, 1–20 (2003).
- <sup>4</sup>S. Grimme, "Semiempirical hybrid density functional with perturbative second-order correlation," *J. Chem. Phys.* **124**, 34108 (2006).

- <sup>5</sup>L. Goerigk and S. Grimme, "Double-hybrid density functionals," *WIREs Comput. Mol. Sci.* **4**, 576–600 (2014).
- <sup>6</sup>N. Mehta, M. Casanova-Páez, and L. Goerigk, "Semi-empirical or non-empirical double-hybrid density functionals: Which are more robust?" *Phys. Chem. Chem. Phys.* **20**, 23175–23194 (2018).
- <sup>7</sup>J. M. L. Martin and G. Santra, "Empirical double-hybrid density functional theory: A 'third way' in between WFT and DFT," *Isr. J. Chem.* **60**, 787–804 (2019).
- <sup>8</sup>Y. Zhang, X. Xu, and W. A. Goddard, "Doubly hybrid density functional for accurate descriptions of nonbond interactions, thermochemistry, and thermochemical kinetics," *Proceedings of the National Academy of Sciences* **106**, 4963–4968 (2009), <https://www.pnas.org/doi/pdf/10.1073/pnas.0901093106>.
- <sup>9</sup>A. D. Becke, G. Santra, and J. M. L. Martin, "A double-hybrid density functional based on good local physics with outstanding performance on the GMTKN55 database," *J. Chem. Phys.* **158**, 151103 (2023).
- <sup>10</sup>M. Kállay, "Linear-scaling implementation of the direct random-phase approximation," *J. Chem. Phys.* **142** (2015).
- <sup>11</sup>J. Shee, M. Loipersberger, A. Rettig, J. Lee, and M. Head-Gordon, "Regularized second-order Møller–Plesset theory: A more accurate alternative to conventional MP2 for noncovalent interactions and transition metal thermochemistry for the same computational cost," *J. Phys. Chem. Lett.* **12**, 12084–12097 (2021).
- <sup>12</sup>G. Santra, E. Semidalas, and J. M. L. Martin, "Exploring avenues beyond revised dsd functionals: II. random-phase approximation and scaled MP3 corrections," *J. Phys. Chem. A* **125**, 4628–4638 (2021).
- <sup>13</sup>G. Santra and J. M. L. Martin, "Do double-hybrid functionals benefit from regularization in the PT2 term? observations from an extensive benchmark," *J. Phys. Chem. Lett.* **13**, 3499–3506 (2022).
- <sup>14</sup>L. Wittmann, H. Neugebauer, S. Grimme, and M. Bursch, "Dispersion-corrected  $r^2$ SCAN based double-hybrid functionals," *J. Chem. Phys.* **159**, 224103 (2023).
- <sup>15</sup>S. Grimme, J. Antony, S. Ehrlich, and H. Krieg, "A consistent and accurate ab initio parametrization of density functional dispersion correction (DFT-D) for the 94 elements H–Pu," *J. Chem. Phys.* **132**, 154104 (2010).
- <sup>16</sup>S. Grimme, S. Ehrlich, and L. Goerigk, "Effect of the Damping Function in Dispersion Corrected Density Functional Theory," *J. Comput. Chem.* **32**, 1456–1465 (2011).
- <sup>17</sup>E. Caldeweyher, S. Ehlert, A. Hansen, H. Neugebauer, S. Spicher, C. Bannwarth, and S. Grimme, "A generally applicable atomic-charge dependent London dispersion correction," *J. Chem. Phys.* **150**, 154122 (2019).
- <sup>18</sup>E. Caldeweyher, C. Bannwarth, and S. Grimme, "Extension of the D3 dispersion coefficient model," *J. Chem. Phys.* **147**, 034112 (2017).
- <sup>19</sup>E. Caldeweyher, J. M. Mewes, S. Ehlert, and S. Grimme, "Extension and evaluation of the D4 London-dispersion model for periodic systems," *Phys. Chem. Chem. Phys.* **22**, 8499–8512 (2020).
- <sup>20</sup>L. Wittmann, I. Gordiy, M. Friede, B. Helmich-Paris, S. Grimme, A. Hansen, and M. Bursch, "Extension of the d3 and d4 london dispersion corrections to the full actinides series," *Physical Chemistry Chemical Physics* (2024), 10.1039/D4CP01514B.
- <sup>21</sup>O. A. Vydrov and T. Van Voorhis, "Nonlocal van der Waals density functional: The simpler the better," *J. Chem. Phys.* **133**, 244103 (2010).
- <sup>22</sup>O. A. Vydrov and T. Van Voorhis, "Nonlocal van der Waals density functional made simple," *Phys. Rev. Lett.* **103**, 063004 (2009).
- <sup>23</sup>W. Hujo and S. Grimme, "Performance of the van der waals density functional VV10 and (hybrid)GGA variants for thermochemistry and noncovalent interactions," *J. Chem. Theory Comput.* **7**, 3866–3871 (2011).
- <sup>24</sup>A. D. Becke and E. R. Johnson, "Exchange-hole dipole moment and the dispersion interaction: High-order dispersion coefficients," *The Journal of Chemical Physics* **124**, 014104 (2006), [https://pubs.aip.org/aip/jcp/article-pdf/doi/10.1063/1.2139668/16657955/014104\\_1\\_online.pdf](https://pubs.aip.org/aip/jcp/article-pdf/doi/10.1063/1.2139668/16657955/014104_1_online.pdf).
- <sup>25</sup>A. D. Becke and E. R. Johnson, "Exchange-hole dipole moment and the dispersion interaction revisited," *The Journal of Chemical Physics* **127**, 154108 (2007), [https://pubs.aip.org/aip/jcp/article-pdf/doi/10.1063/1.2795701/15404406/154108\\_1\\_online.pdf](https://pubs.aip.org/aip/jcp/article-pdf/doi/10.1063/1.2795701/15404406/154108_1_online.pdf).
- <sup>26</sup>A. D. Becke and E. R. Johnson, "A density-functional model of the dispersion interaction," *The Journal of Chemical Physics* **123**, 154101 (2005), [https://pubs.aip.org/aip/jcp/article-pdf/doi/10.1063/1.2065267/13408810/154101\\_1\\_online.pdf](https://pubs.aip.org/aip/jcp/article-pdf/doi/10.1063/1.2065267/13408810/154101_1_online.pdf).
- <sup>27</sup>E. R. Johnson and A. D. Becke, "A post-Hartree-Fock model of intermolecular interactions: Inclusion of higher-order corrections," *The Journal of Chemical Physics* **124**, 174104 (2006), [https://pubs.aip.org/aip/jcp/article-pdf/doi/10.1063/1.2190220/15384605/174104\\_1\\_online.pdf](https://pubs.aip.org/aip/jcp/article-pdf/doi/10.1063/1.2190220/15384605/174104_1_online.pdf).
- <sup>28</sup>A. Tkatchenko and M. Scheffler, "Accurate Molecular Van Der Waals Interactions from Ground-State Electron Density and Free-Atom Reference Data," *Phys. Rev. Lett.* **102**, 073005 (2009).
- <sup>29</sup>A. Tkatchenko, R. A. DiStasio, R. Car, and M. Scheffler, "Accurate and Efficient Method for Many-Body van der Waals Interactions," *Phys. Rev. Lett.* **108**, 236402 (2012).
- <sup>30</sup>M. Bursch, E. Caldeweyher, A. Hansen, H. Neugebauer, S. Ehlert, and S. Grimme, "Understanding and Quantifying London Dispersion Effects in Organometallic Complexes," *Acc. Chem. Res.* **52**, 258–266 (2019).
- <sup>31</sup>S. Grimme, F. Bohle, A. Hansen, P. Pracht, S. Spicher, and M. Stahn, "Efficient Quantum Chemical Calculation of Structure Ensembles and Free Energies for Nonrigid Molecules," *J. Phys. Chem. A* **125**, 4039–4054 (2021).
- <sup>32</sup>N. Jacob, Y. Zaid, J. C. A. Oliveira, L. Ackermann, and J. Wencel-Delord, "Cobalt-catalyzed enantioselective c–h arylation of indoles," *J. Am. Chem. Soc.* **144**, 798–806 (2022).
- <sup>33</sup>S. Grimme and P. R. Schreiner, "The role of london dispersion interactions in modern chemistry," *Accounts of Chemical Research* **57**, 2233–2233 (2024).
- <sup>34</sup>R. C. Lochan, Y. Jung, and M. Head-Gordon, "Scaled opposite spin second order Møller-Plesset theory with improved physical description of long-range dispersion interactions," *J. Phys. Chem. A* **109**, 7598–7605 (2005).
- <sup>35</sup>Y. Jung, R. C. Lochan, A. D. Dutoi, and M. Head-Gordon, "Scaled opposite-spin second order moller-pletset correlation energy: An economical electronic structure method," *J. Chem. Phys.* **121**, 9793–9802 (2004).
- <sup>36</sup>S. Grimme, "Semiempirical hybrid density functional with perturbative second-order correlation," *J. Chem. Phys.* **124**, 034108 (2006).
- <sup>37</sup>A. Görling and M. Levy, "Exact kohn-sham scheme based on perturbation theory," *Physical Review A* **50**, 196 (1994).
- <sup>38</sup>G. Santra, M. Cho, and J. M. L. Martin, "Exploring avenues beyond revised dsd functionals: I. range separation, with xdsd as a special case," *J. Phys. Chem. A* **125**, 4614–4627 (2021).
- <sup>39</sup>S. Kozuch, D. Gruzman, and J. M. L. Martin, "DSD-BLYP: A General Purpose Double Hybrid Density Functional Including Spin Component Scaling and Dispersion Correction," *J. Phys. Chem. C* **114**, 20801–20808 (2010).
- <sup>40</sup>S. Kozuch and J. M. L. Martin, "DSD-PBEP86: in search of the best double-hybrid DFT with spin-component scaled MP2 and dispersion corrections," *Phys. Chem. Chem. Phys.* **13**, 20104–20107 (2011).
- <sup>41</sup>S. Kozuch and J. M. L. Martin, "Spin-component-scaled double hybrids: An extensive search for the best fifth-rung functionals blending dft and perturbation theory," *J. Comput. Chem.* **34**, 2327–2344 (2013).
- <sup>42</sup>M. K. Kesharwani, B. Brauer, and J. M. L. Martin, "Frequency and zero-point vibrational energy scale factors for double-hybrid density functionals (and other selected methods): Can anharmonic force fields be avoided?" *J. Phys. Chem. A* **119**, 1701–1714 (2015).
- <sup>43</sup>G. Santra, N. Sylvetsky, and J. M. Martin, "Minimally empirical double-hybrid functionals trained against the GMTKN55 database: revDSD-PBEP86-D4, revDOD-PBE-D4, and DOD-SCAN-D4," *J. Phys. Chem. A* **123**, 5129–5143 (2019).
- <sup>44</sup>N. Mehta, G. Santra, and J. M. Martin, "Is explicitly correlated double-hybrid density functional theory advantageous for vibrational frequencies?" *Canadian Journal of Chemistry* **101**, 656–663 (2023).
- <sup>45</sup>M. K. Kesharwani, S. Kozuch, and J. M. L. Martin, "Comment on 'Doubly hybrid density functional xDH-PBE0 from a parameter-free global hybrid model PBE0' [*J. Chem. Phys.* 136, 174103 (2012)]," *J. Chem. Phys.* **143**, 187101 (2015).
- <sup>46</sup>G. Santra, E. Semidalas, and J. M. L. Martin, "Surprisingly good performance of XYG3 family functionals using a scaled KS-MP3 correlation," *J. Phys. Chem. Lett.* **12**, 9368–9376 (2021).
- <sup>47</sup>Y. Zhang, X. Xu, and W. A. Goddard, "Doubly hybrid density functional for accurate descriptions of nonbonded interactions, thermochemistry, and thermochemical kinetics," *Proc. Natl. Acad. Sci. U. S. A.* **106**, 4963–4968 (2009).

- <sup>48</sup>I. Y. Zhang, N. Q. Su, É. A. G. Brémond, C. Adamo, and X. Xu, "Doubly hybrid density functional xDH-PBE0 from a parameter-free global hybrid model PBE0," *J. Chem. Phys.* **136**, 174103 (2012).
- <sup>49</sup>L. Goerigk and S. Grimme, "A thorough benchmark of density functional methods for general main group thermochemistry, kinetics, and noncovalent interactions," *Phys. Chem. Chem. Phys.* **13**, 6670–6688 (2011).
- <sup>50</sup>I. Y. Zhang, X. Xu, Y. Jung, and W. A. Goddard, "A fast doubly hybrid density functional method close to chemical accuracy using a local opposite spin ansatz," *Proc. Natl. Acad. Sci. U. S. A.* **108**, 19896–19900 (2011).
- <sup>51</sup>I. Y. Zhang and X. Xu, "Reaching a uniform accuracy for complex molecular systems: long-range-corrected XYG3 doubly hybrid density functional," *J. Phys. Chem. Lett.* **4**, 1669–1675 (2013).
- <sup>52</sup>I. Y. Zhang and X. Xu, "Exploring the limits of the XYG3-type doubly hybrid approximations for the main-group chemistry: The xDH@B3LYP model," *J. Phys. Chem. Lett.* **12**, 2638–2644 (2021).
- <sup>53</sup>G. Santra, M. Cho, and J. M. L. Martin, "Correction to 'exploring avenues beyond revised DSD functionals: I. range separation, with xDSD as a special case'," *J. Phys. Chem. A* **128**, 974–975 (2024).
- <sup>54</sup>B. Axilrod and E. Teller, "Interaction of the van der waals type between three atoms," *J. Chem. Phys.* **11**, 299–300 (1943).
- <sup>55</sup>Y. Muto, "Force between nonpolar molecules," *J. Phys. Math. Soc. Jpn* **17**, 629–631 (1943).
- <sup>56</sup>E. Epifanovsky, A. T. B. Gilbert, X. Feng, J. Lee, Y. Mao, N. Mardirossian, P. Pokhilko, A. F. White, M. P. Coons, A. L. Dempwolff, Z. Gan, D. Hait, P. R. Horn, L. D. Jacobson, I. Kaliman, J. Kussmann, A. W. Lange, K. U. Lao, D. S. Levine, J. Liu, S. C. McKenzie, A. F. Morrison, K. D. Nanda, F. Plasser, D. R. Rehn, M. L. Vidal, Z.-Q. You, Y. Zhu, B. Alam, B. J. Albrecht, A. Aldossary, E. Alguire, J. H. Andersen, V. Athavale, D. Barton, K. Begam, A. Behn, N. Bellonzi, Y. A. Bernard, E. J. Berquist, H. G. A. Burton, A. Carreras, K. Carter-Fenk, R. Chakraborty, A. D. Chien, K. D. Closser, V. Cofer-Shabica, S. Dasgupta, M. de Wergifosse, J. Deng, M. Diedenhofen, H. Do, S. Ehlert, P.-T. Fang, S. Fatehi, Q. Feng, T. Friedhoff, J. Gayvert, Q. Ge, G. Gidofalvi, M. Goldey, J. Gomes, C. E. González-Espinoza, S. Gulania, A. O. Gunina, M. W. D. Hanson-Heine, P. H. P. Harbach, A. Hauser, M. F. Herbst, M. Hernández Vera, M. Hodecker, Z. C. Holden, S. Houck, X. Huang, K. Hui, B. C. Huynh, M. Ivanov, Á. Jász, H. Ji, H. Jiang, B. Kaduk, S. Kähler, K. Khistyayev, J. Kim, G. Kis, P. Klunzinger, Z. Koczor-Benda, J. H. Koh, D. Kosenkov, L. Koulias, T. Kowalczyk, C. M. Krauter, K. Kue, A. Kunitsa, T. Kus, I. Ladžánszki, A. Landau, K. V. Lawler, D. Lefrançois, S. Lehtola, R. R. Li, Y.-P. Li, J. Liang, M. Liebenthal, H.-H. Lin, Y.-S. Lin, F. Liu, K.-Y. Liu, M. Loipersberger, A. Luenser, A. Manjanath, P. Manohar, E. Mansoor, S. F. Manzer, S.-P. Mao, A. V. Marenich, T. Markovich, S. Mason, S. A. Maurer, P. F. McLaughlin, M. F. S. J. Menger, J.-M. Mewes, S. A. Mewes, P. Morgante, J. W. Mullinax, K. J. Oosterbaan, G. Paran, A. C. Paul, S. K. Paul, F. šević, Z. Pei, S. Prager, E. I. Proynov, Á. Rák, E. Ramos-Cordoba, B. Rana, A. E. Rask, A. Rettig, R. M. Richard, F. Rob, E. Rossomme, T. Scheele, M. Scheurer, N. Schneider, N. Sergueev, S. M. Sharada, W. Skomorowski, D. W. Small, C. J. Stein, Y.-C. Su, E. J. Sundstrom, Z. Tao, J. Thirman, G. J. Tornai, T. Tsuchimochi, N. M. Tubman, S. P. Veccham, O. Vydrov, J. Wenzel, J. Witte, A. Yamada, K. Yao, S. Yeganeh, S. R. Yost, A. Zech, I. Y. Zhang, X. Zhang, Y. Zhang, D. Zuev, A. Aspuru-Guzik, A. T. Bell, N. A. Besley, K. B. Bravaya, B. R. Brooks, D. Casanova, J.-D. Chai, S. Coriani, C. J. Cramer, G. Cserey, I. DePrince, A. Eugene, J. DiStasio, Robert A., A. Dreuw, B. D. Dunietz, T. R. Furlani, I. Goddard, William A., S. Hammes-Schiffer, T. Head-Gordon, W. J. Hehre, C.-P. Hsu, T.-C. Jagau, Y. Jung, A. Klamt, J. Kong, D. S. Lambrecht, W. Liang, N. J. Mayhall, C. W. McCurdy, J. B. Neaton, C. Ochsenfeld, J. A. Parkhill, R. Peverati, V. A. Rassolov, Y. Shao, L. V. Slipchenko, T. Stauch, R. P. Steele, J. E. Subotnik, A. J. W. Thom, A. Tkatchenko, D. G. Truhlar, T. Van Voorhis, T. A. Wesolowski, K. B. Whaley, I. Woodcock, H. Lee, P. M. Zimmerman, S. Faraji, P. M. W. Gill, M. Head-Gordon, J. M. Herbert, and A. I. Krylov, "Software for the frontiers of quantum chemistry: An overview of developments in the q-chem 5 package," *J. Chem. Phys.* **155**, 084801 (2021).
- <sup>57</sup>F. Weigend and R. Ahlrichs, "Balanced basis sets of split valence, triple zeta valence and quadruple zeta valence quality for H to Rn: Design and assessment of accuracy," *Phys. Chem. Chem. Phys.* **7**, 3297 (2005).
- <sup>58</sup>V. S. Bryantsev, M. S. Diallo, A. C. T. van Duin, and W. A. I. Goddard, "Evaluation of B3LYP, X3LYP, and M06-Class Density Functionals for Predicting the Binding Energies of Neutral, Protonated, and Deprotonated Water Clusters," *J. Chem. Theory Comput* **5**, 1016–1026 (2009).
- <sup>59</sup>L. Goerigk, A. Hansen, C. Bauer, S. Ehrlich, A. Najibi, and S. Grimme, "A look at the density functional theory zoo with the advanced GMTKN55 database for general main group thermochemistry, kinetics and noncovalent interactions," *Phys. Chem. Chem. Phys.* **19**, 32184–32215 (2017).
- <sup>60</sup>K. U. Lao, R. Schäffer, G. Jansen, and J. M. Herbert, "Accurate description of intermolecular interactions involving ions using symmetry-adapted perturbation theory," *J. Chem. Theory Comput* **11**, 2473–2486 (2015).
- <sup>61</sup>L. A. Curtiss, K. Raghavachari, G. W. Trucks, and J. A. Pople, "Gaussian-2 theory for molecular energies of first- and second-row compounds," *J. Chem. Phys.* **94**, 7221–7230 (1991).
- <sup>62</sup>Y. Zhao, B. J. Lynch, and D. G. Truhlar, "Multi-coefficient extrapolated density functional theory for thermochemistry and thermochemical kinetics," *Phys. Chem. Chem. Phys.* **7**, 43–52 (2005).
- <sup>63</sup>Y. Zhao, N. González-García, and D. G. Truhlar, "Benchmark database of barrier heights for heavy atom transfer, nucleophilic substitution, association, and unimolecular reactions and its use to test theoretical methods," *J. Phys. Chem. A* **109**, 2012–2018 (2005).
- <sup>64</sup>L. Goerigk and S. Grimme, "A general database for main group thermochemistry, kinetics, and noncovalent interactions – assessment of common and reparameterized (meta-)gga density functionals," *Journal of Chemical Theory and Computation* **6**, 107–126 (2010).
- <sup>65</sup>D. Rappoport and F. Furche, "Property-optimized Gaussian basis sets for molecular response calculations," *J. Chem. Phys.* **133**, 134105 (2010).
- <sup>66</sup>D. Andrae, U. Häußermann, M. Dolg, H. Stoll, and H. Preuß, "Energy-Adjusted *ab initio* Pseudopotentials for the Second and Third Row Transition Elements," *Theor. Chim. Acta* **77**, 123–141 (1990).
- <sup>67</sup>K. A. Peterson, D. Figgen, E. Goll, H. Stoll, and M. Dolg, "Systematically Convergent Basis Sets with Relativistic Pseudopotentials. II. Small-Core Pseudopotentials and Correlation Consistent Basis Sets for the Post-*d* Group 16–18 Elements," *J. Chem. Phys.* **119**, 11113–11123 (2003).
- <sup>68</sup>C. Hättig, "Optimization of auxiliary basis sets for ri-mp2 and ri-cc2 calculations: Core-valence and quintuple- $\zeta$  basis sets for h to ar and qzvpp basis sets for li to kr," *Phys. Chem. Chem. Phys.* **7**, 59–66 (2005).
- <sup>69</sup>A. Hellweg and D. Rappoport, "Development of new auxiliary basis functions of the karlsruhe segmented contracted basis sets including diffuse basis functions (def2-svpd, def2-tzvpd, and def2-qvppd) for ri-mp2 and ri-cc calculations," *Phys. Chem. Chem. Phys.* **17**, 1010–1017 (2015).
- <sup>70</sup>S. Dasgupta and J. M. Herbert, "Standard grids for high-precision integration of modern density functionals: Sg-2 and sg-3," *J. Comput. Chem* **38**, 869–882 (2017).
- <sup>71</sup>J. Sun, A. Ruzsinszky, and J. P. Perdew, "Strongly constrained and appropriately normed semilocal density functional," *Phys. Rev. Lett.* **115**, 036402 (2015).
- <sup>72</sup>J. G. Brandenburg, J. E. Bates, J. Sun, and J. P. Perdew, "Benchmark tests of a strongly constrained semilocal functional with a long-range dispersion correction," *Phys. Rev. B* **94**, 115144 (2016).
- <sup>73</sup>M. Kállay, P. R. Nagy, D. Mester, Z. Rolik, G. Samu, J. Csontos, J. Csóka, P. B. Szabó, L. Gyevi-Nagy, B. Hégyel, I. Ladžánszki, L. Szegedy, B. Ladóczki, K. Petrov, M. Farkas, P. D. Mezei, and Á. Ganyecz, "The mrc program system: Accurate quantum chemistry from water to proteins," *J. Chem. Phys.* **152** (2020).
- <sup>74</sup>B. Chan, "Assessment and development of DFT with the expanded CUAGAU-2 set of group-11 cluster systems," *Int. J. Quantum Chem.* **121**, e26453 (2021).
- <sup>75</sup>R. Kang, W. Lai, J. Yao, S. Shaik, and H. Chen, "How accurate can a local coupled cluster approach be in computing the activation energies of late-transition-metal-catalyzed reactions with Au, Pt, and Ir?" *J. Chem. Theory Comput.* **8**, 3119–3127 (2012).
- <sup>76</sup>M. A. Iron and T. Janes, "Evaluating Transition Metal Barrier Heights with the Latest Density Functional Theory Exchange-Correlation Functionals: The MOBH35 Benchmark Database," *J. Phys. Chem. A* **123**, 3761–3781 (2019).
- <sup>77</sup>M. A. Iron and T. Janes, "Correction to 'Evaluating Transition Metal Barrier Heights with the Latest Density Functional Theory Exchange-Correlation Functionals: The MOBH35 Benchmark Database'," *J. Phys. Chem. A* **123**, 3761–3781 (2019).
- <sup>78</sup>S. Dohm, M. Bursch, A. Hansen, and S. Grimme, "Semiautomated Transition State Localization for Organometallic Complexes with Semiempirical

- Quantum Chemical Methods,” *J. Chem. Theory Comput.* **16**, 2002–2012 (2020).
- <sup>79</sup>S. Dohm, A. Hansen, M. Steinmetz, S. Grimme, and M. P. Checinski, “Comprehensive Thermochemical Benchmark Set of Realistic Closed-Shell Metal Organic Reactions,” *J. Chem. Theory Comput.* **14**, 2596–2608 (2018).
- <sup>80</sup>L. R. Maurer, M. Bursch, S. Grimme, and A. Hansen, “Assessing Density Functional Theory for Chemically Relevant Open-Shell Transition Metal Reactions,” *J. Chem. Theory Comput.* **17**, 6134–6151 (2021).
- <sup>81</sup>Y. Sun and H. Chen, “Performance of Density Functionals for Activation Energies of Re-Catalyzed Organic Reactions,” *J. Chem. Theory Comput.* **10**, 579–588 (2014).
- <sup>82</sup>Y. Sun and H. Chen, “Performance of density functionals for activation energies of Zr-mediated reactions,” *J. Chem. Theory Comput.* **9**, 4735–4743 (2013).
- <sup>83</sup>Y. Sun, L. Hu, and H. Chen, “Comparative Assessment of DFT Performances in Ru- and Rh-Promoted  $\sigma$ -Bond Activations,” *J. Chem. Theory Comput.* **11**, 1428–1438 (2015).
- <sup>84</sup>L. Hu and H. Chen, “Assessment of DFT Methods for Computing Activation Energies of Mo/W-Mediated Reactions,” *J. Chem. Theory Comput.* **11**, 4601–4614 (2015).
- <sup>85</sup>M. Bursch, A. Hansen, P. Pracht, J. T. Kohn, and S. Grimme, “Theoretical study on conformational energies of transition metal complexes,” *Phys. Chem. Chem. Phys.* **23**, 287–299 (2021).
- <sup>86</sup>B. Rudshcheyn, J. L. Weber, D. Coskun, P. A. Devlaminck, S. Zhang, D. R. Reichman, J. Shee, and R. A. Friesner, “Calculation of Metallocene Ionization Potentials via Auxiliary Field Quantum Monte Carlo: Toward Benchmark Quantum Chemistry for Transition Metals,” *J. Chem. Theory Comput.* **18**, 2845–2862 (2021).
- <sup>87</sup>T. Husch, L. Freitag, and M. Reiher, “Calculation of Ligand Dissociation Energies in Large Transition-Metal Complexes,” *J. Chem. Theory Comput.* **14**, 2456–2468 (2018).
- <sup>88</sup>T. Husch, L. Freitag, and M. Reiher, “Correction to: ‘Calculation of ligand dissociation energies in large transition-metal complexes’ (*J. Chem. Theory Comput.* (2018) 14:5 (2456–2468) DOI: 10.1021/acs.jctc.8b00061),” *J. Chem. Theory Comput.* **15**, 4295–4296 (2019).
- <sup>89</sup>P. J. Huber, *Robust statistics*, Vol. 523 (John Wiley & Sons, 2004).
- <sup>90</sup>R. C. Geary, “The ratio of the mean deviation to the standard deviation as a test of normality,” *Biometrika* **27**, 310–332 (1935).
- <sup>91</sup>M. J. Powell, “The bobyqa algorithm for bound constrained optimization without derivatives,” Cambridge NA Report NA2009/06, University of Cambridge, Cambridge **26** (2009).
- <sup>92</sup>A. Karton, S. Daon, and J. M. Martin, “W4-11: A high-confidence benchmark dataset for computational thermochemistry derived from first-principles W4 data,” *Chem. Phys. Lett.* **510**, 165–178 (2011).
- <sup>93</sup>D. Řeha, H. Valdés, J. Vondrášek, P. Hobza, A. Abu-Riziq, B. Crews, and M. S. de Vries, “Structure and ir spectrum of phenylalanyl-glycyl-glycine tripeptide in the gas-phase: Ir/uv experiments, ab initio quantum chemical calculations, and molecular dynamic simulations,” *Chem. – Eur. J.* **11**, 6803–6817 (2005).
- <sup>94</sup>L. Goerigk, A. Karton, J. M. L. Martin, and L. Radom, “Accurate quantum chemical energies for tetrapeptide conformations: why mp2 data with an insufficient basis set should be handled with caution,” *Phys. Chem. Chem. Phys.* **15**, 7028–7031 (2013).
- <sup>95</sup>J. Řezáč, K. E. Riley, and P. Hobza, “S66: A well-balanced database of benchmark interaction energies relevant to biomolecular structures,” *J. Chem. Theory Comput.* **7**, 2427–2438 (2011).
- <sup>96</sup>F. Neese, T. Schwabe, S. Kossmann, B. Schirmer, and S. Grimme, “Assessment of orbital-optimized, spin-component scaled second-order many-body perturbation theory for thermochemistry and kinetics,” *J. Chem. Theory Comput.* **5**, 3060–3073 (2009).
- <sup>97</sup>S. N. Steinmann, G. Csonka, and C. Corminboeuf, “Unified inter- and intramolecular dispersion correction formula for generalized gradient approximation density functional theory,” *J. Chem. Theory Comput.* **5**, 2950–2958 (2009).
- <sup>98</sup>H. Kriegel and S. Grimme, “Thermochemical benchmarking of hydrocarbon bond separation reaction energies: Jacob’s ladder is not reversed!” *Mol. Phys.* **108**, 2655–2666 (2010).
- <sup>99</sup>D. H. Ess and K. N. Houk, “Activation energies of pericyclic reactions: Performance of dft, mp2, and cbs-qb3 methods for the prediction of activation barriers and reaction energetics of 1,3-dipolar cycloadditions, and revised activation enthalpies for a standard set of hydrocarbon pericyclic reactions,” *J. Phys. Chem. A* **109**, 9542–9553 (2005).
- <sup>100</sup>V. Guner, K. S. Khuong, A. G. Leach, P. S. Lee, M. D. Bartberger, and K. N. Houk, “A standard set of pericyclic reactions of hydrocarbons for the benchmarking of computational methods: The performance of ab initio, density functional, cbscf, caspt2, and cbs-qb3 methods for the prediction of activation barriers, reaction energetics, and transition state geometries,” *J. Phys. Chem. A* **107**, 11445–11459 (2003).
- <sup>101</sup>T. C. Dinadayalane, R. Vijaya, A. Smitha, and G. N. Sastry, “Diels-alder reactivity of butadiene and cyclic five-membered dienes ((ch)<sub>4</sub>x, x = ch<sub>2</sub>, sih<sub>2</sub>, o, nh, ph, and s) with ethylene: A benchmark study,” *J. Phys. Chem. A* **106**, 1627–1633 (2002).
- <sup>102</sup>H. Neugebauer, H. T. Vuong, J. L. Weber, R. A. Friesner, J. Shee, and A. Hansen, “Toward benchmark-quality ab initio predictions for 3d transition metal electrocatalysts: A comparison of ccscd(t) and ph-afqmc,” *Journal of Chemical Theory and Computation* **19**, 6208–6225 (2023).
- <sup>103</sup>G. Santra, M. Cho, and J. M. Martin, “Exploring Avenues beyond Revised DSD Functionals: I. Range Separation, with xDSD as a Special Case,” *J. Phys. Chem. A* **125**, 4614–4627 (2021).